VOL.40 Nº3 2023
https://doi.org/10.22491/rmct.v40i3.11676.en

Development of a radio frequency magnetron sputtering system for the production of thin films

Austim Mota Gomide Pimenta[1] and Carlos Ferreira[1]
[1]Materials Engineering Teaching Section – SE/8, Military Institute of Engineering, Rio de Janeiro, Brazil,
austimpimenta@gmail.com
argus@ime.eb.br

ABSTRACT: This work describes the design, construction and characterization of a radio frequency magnetron sputtering system for thin film deposition. Target-materials with different electrical properties were used for system characterization: copper, indium oxide and silicon dioxide. The films were deposited on glass and silicon substrates, at room temperature, under a pressure of 8x10-4 Torr. The microstructure of the obtained thin films was investigated by X-ray diffraction and atomic force microscopy. Electrical and optical properties were obtained by Hall effect and transmittance measurements, respectively. The results showed that the assembled sputtering system allows the deposition of high quality films with high thickness uniformity. Linear dependence of the deposition rate on the work power was achieved for the deposited films, whose properties were well consistent with those reported in the literature. These results show the control of deposition parameters in the assembled system.

KEYWORDS: Instrumentation. RF Magnetron Sputtering. Thin Films. Structural Properties. Electrical Properties. Optical Properties.

RESUMO: Este trabalho descreve a concepção, a construção e a caracterização de um sistema de pulverização catódica com fonte de radiofrequência assistida por campos magnéticos para deposição de filmes finos. Materiais para alvo com propriedades elétricas distintas, foram usados para caracterizar o sistema: cobre, óxido de índio e dióxido de silício. Os filmes foram depositados em substratos de vidro e silício, à temperatura ambiente, com uma pressão de deposição da ordem de 8x10^{-4} Torr. A microestrutura dos filmes finos obtidos foi caracterizada por difração de raios x e microscopia de força atômica. As propriedades elétricas e óticas foram obtidas pelas medidas de efeito Hall e de transmitância, respectivamente. Os resultados mostraram que o sistema construído possibilita a deposição de filmes de alta qualidade e boa uniformidade de espessura. Para todos os materiais investigados, a taxa de deposição aumentou linearmente com a potência e as propriedades obtidas estavam de acordo com os valores reportados na literatura, mostrando o controle dos parâmetros de deposição no sistema construído.

PALAVRAS-CHAVE: Instrumentação. Pulverização Catódica. Filmes Finos. Propriedades Estruturais. Propriedades Elétricas. Propriedades Ópticas.

1. Introduction

Theoretical advances in the various fields of science impose the need to establish mastery of techniques and improvement of equipment assembly skills, in such a way that the branch of scientific instrumentation is essential for developing the various areas of science. In recent decades, thin film deposition techniques have stood out due to their applications, both in industry and in various fields of science [1]. The production of materials, in the form of thin films by sputtering, stands out for the ability to manufacture thin films of materials with complex compositions, at room temperature, regardless of their electrical, optical, and mechanical properties [2, 3, 4].

This study's objective is to present the design and construction of a system for the deposition of thin films by sputtering with a radio frequency source assisted by magnetic fields (RF Magnetron Sputtering), for the manufacture of thin films. To prove the success of the assembled system, thin films of materials with different electrical properties were deposited: copper, as an electrically conductive material, silicon dioxide, as an electrical insulating material, and indium oxide, with semiconductor properties. Finally, the thin films produced were characterized to prove their quality as well as the technical feasibility of the assembled equipment.

2. Materials and Methods

2.1 Development of the Magnetron Sputtering System Project

For the project assembly, a stainless-steel cylindrical bell jar, measuring 30 cm in diameter and 30

cm in height, was used for the deposition chamber. It was evacuated by a system consisting of a diffusion pump with a cryogenic trap to obtain high vacuum, a dry scroll vacuum pump to obtain primary vacuum, a valve with controlled opening for the pumping conductance during deposition, and a set of pressure gauges. The assembly of the projected deposition system was divided into stages:

- (i) Dimensioning and assembly of a cabinet to support the bell jar and gauges, using angle brackets of carbon steel, and aluminum plates to support the equipment and its closure. An aluminum plate was placed at the top of the cabinet to support the deposition chamber, and another aluminum plate was placed at the bottom to support the pumping system. Figure 1 illustrates the equipment structural design;
- (ii) Use of a 306L stainless-steel cylindrical disc to support the internal components of the deposition system (base plate);
- (iii) Design of the electrical power system, enabling the independent supply of the electronic equipment that comprise the deposition system and the performance of individual tests in each part of the electrical system, both in the vacuum pumping system and in the radio frequency and instrumentation equipment;
- (iv) Resizing and adaptation of the pre-existing vacuum system at the Laboratory of the Thin Film (LFF) of the Military Institute of Engineering (IME) (Figure 2);
- (v) Sizing and installation of the forced air-cooling system with cold water for the diffusion pump, and for the target material for deposition;
- (vi) Assembly and installation of a shutter to protect the substrates during the stage of removal of impurities affixed to the target surface, and in the stage of control of deposition rate and film thickness;
- (vii) Installation of a stainless-steel square as a substrate holder with 10 cm edge, with adjustable height, to accommodate four square substrates of 2.5 cm;
- (viii) Installation of a RFX 600 radio frequency generation source, and an ATX module of automatic impedance-matching for the substrate-cathode, both manufactured by Advanced Energy;
- (xix) Installation of a magnetron cathode, model MAK3, manufactured by MEIVAC, which holds 3-inch diameter targets;
- (x) Installation of a pressure gauge with capacitive membrane, manufactured by EDWARDS (Barocel® model 600A-100T-R12-N12X-4), to evaluate the base pressure of the system, and a cold cathode ionization gauge, manufactured by EDWARDS (Penning®, model 6 D145-08-00), for evaluation of the high vacuum;
- (xi) Installation of a pressure gauge with capacitive membrane, model 626ª01TDE manufactured by MKS, for pressure measurement during deposition;
- (xii) Installation of a needle valve, model SS-4-BK manufactured by Swagelok®, to control the flow of argon in the chamber during the purging and deposition stages.

The designed and assembled system is shown in Figure 3.

Fig. 1 - Schematic representation of the support cabinet in exploded-view drawing.

Fig. 2 - a) High vacuum system; b) Schematic of the vacuum system in exploded-view drawing.

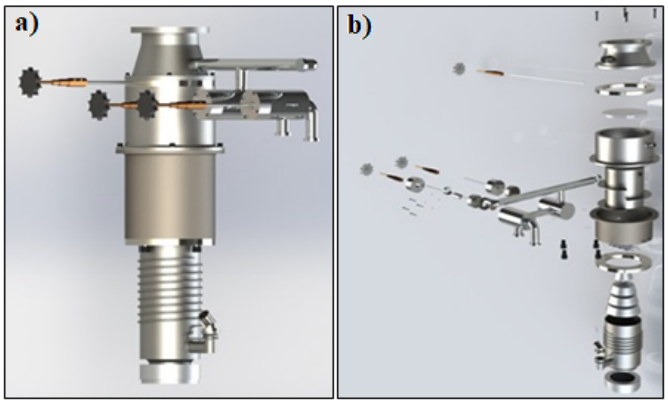

Fig. 3 - a) Design of the sputtering system; b) Photograph of the sputtering system assembled.

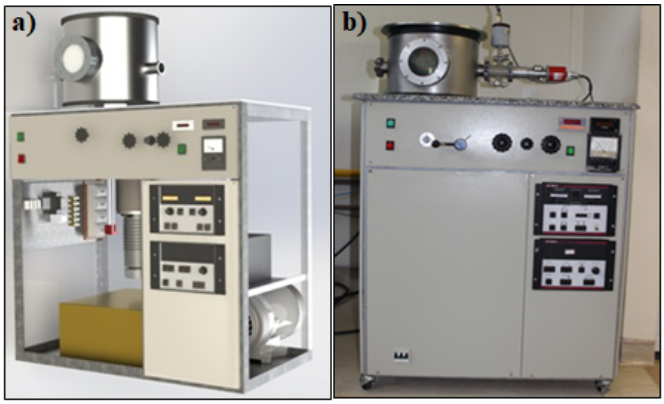

2.2 Characterization of the deposition system

To characterize the deposition system initially assembled, thin films deposited on glass slides and on monocrystalline silicon chips were produced.

Before sample production, the system was pumped up to a base pressure of $8x10^{-6}$ Torr, followed by the stage of obtaining an argon residual atmosphere. This step was performed with the following experimental procedure: a first purge was performed by injecting argon into the deposition chamber, using the needle valve to raise the pressure up to 3 mTorr. The pressure was maintained for about 60s; subsequently, the pressure was reduced to the base pressure by closing the needle valve. This procedure was performed at least three times to ensure that the argon residual atmosphere was obtained. Finally, the pressure was maintained at 3 mTorr to perform the deposition.

For the production of a full series of samples, copper, silicon dioxide, and indium oxide targets were used. The films were deposited on glass slides and with different power outputs to characterize the deposition system. Table 1 presents the deposition parameters used, kept constant during the production of the films, regardless of the type of target material used.

Table 1 - Parameters kept constant during depositions.

Parameters	Values
System Base Pressure	~$8x10^{-6}$ Torr
Plasma opening pressure	30 mTorr
Deposition pressure	1 mTorr
Target-substrate distance	75 mm
Deposition temperature	Ambient

After the production of the thin films, thickness was measured using the Veeco profilometer, model Dektak 150 of the LFF, and the Dektak 8 from the Materials Division (Dimat) of INMETRO. To obtain electrical resistivity, the LFF BioRad equipment model HL 5500 was used. For structural characterization of the deposited films, the X'Pert Powder diffractometer of PANalytical, from the Laboratory of X-ray Diffraction of IME, was used. For morphological analysis, a Witec atomic force microscopy (AFM), model Alpha 300 from Dimat/INMETRO, and the high-resolution scanning electron microscope, model HELIOS NANOLAB, FEI trademark installed at the Microscopy Center of INMETRO, were used.

3. Results

The copper target was the first material used to manufacture the films, followed by the silicon dioxide target, due to its opposite electrical properties. The other material used for the characterization of the deposition system was indium oxide, for its semiconduc-

tor characteristic. Tables 2 to 4 present the deposition parameters used, with the values obtained for thickness, deposition rate, and resistivity of films (since SiO_2 films are insulating, they could not be measured for resistivity). The deposition time was maintained at 10 min for copper depositions and 60 min for SiO_2 and In_2O_3 depositions. The deposition pressure was maintained at 1 mTorr for all depositions. Due to the insulating characteristic of silicon dioxide, it was necessary to apply higher power outputs to enable film production with deposition rates in the same range as those used in copper and In_2O_3 targets.

Table 2 - Thickness and resistivity of thin films of copper in function of deposition parameters.

Film	Power (W)	Thickness (Å)	Rate (Å/s)	Resistivity (μΩ.cm)
1	20	393	0.7	0.1
2	50	1366	2.3	1.6
3	80	2445	4.1	0.6
4	110	3850	6.4	3.6

Table 3 - Thickness and resistivity of thin films of SiO_2 in function of deposition parameters.

Film	Power (W)	Thickness (Å)	Rate (Å/s)
1	100	3396	0.9
2	150	6266	1.7
3	200	9125	2.5

Table 4 - Thickness and resistivity of thin films of In_2O_3 in function of deposition parameters.

Film	Power (W)	Thickness (Å)	Rate (Å/s)	Resistivity (μΩ.cm)
1	20	2265	0.6	131
2	50	5272	1.4	138
3	80	10152	2.8	195
4	110	14282	3.9	120

Figure 4 shows the behavior of the deposition rate in function of the power used to produce the films. Analyzing Figure 4, it is possible to observe the existence of a very strong linear correlation between the deposition rate of the three materials used and the work power. This result is well known in the literature [5-7] and attests to the control of this important deposition parameter in the assembled system.

Fig. 4 - Deposition rate of thin films manufactured in the sputtering system in function of power: a) copper; b) SiO_2, and c) In_2O_3.

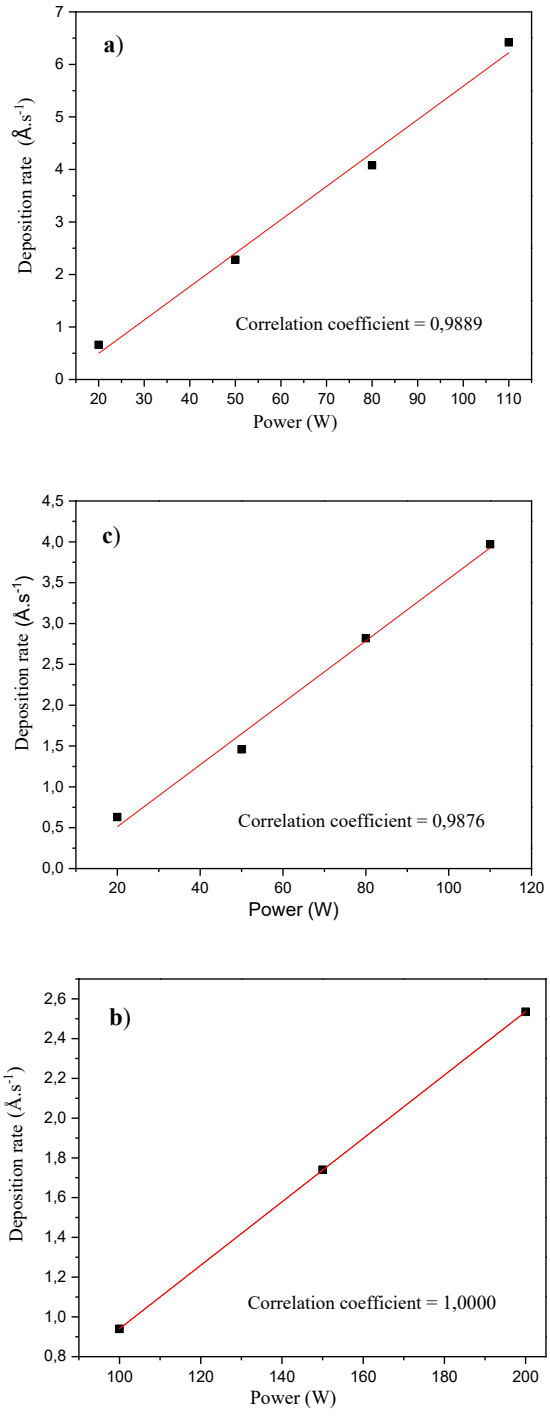

Figure 5 shows the diffractograms of the deposited films at different power outputs. It is important to highlight the absence of contaminating phases in the deposited films, which attest to this system capacity of depositing pure and good quality films.

In the case of copper films, it is observed that the films deposited with the powers of 50, 80, and 110W are crystalline and show a preferential growth in the direction (111), according to the crystallographic data JCPDS 00-004-0836 of copper. It is also observed that the thin film deposited with 110W has higher crystallinity than the others, while the copper thin film deposited with 20W is amorphous. The crystallinity resulting from the work power increase is possibly related to the greater number of atoms that reach the substrate per time interval, favoring the increase in the thickness of films and, consequently, the crystallinity. The amorphous characteristic of the film deposited with 20 W is due to the low deposition rate used (0.7 Å/s) resulting in a small thickness, when compared to other films.

Degrees
Deposition power (W)

Analyzing the diffractograms of SiO_2 films, it is possible to observe that all films are amorphous. This result is well known and related to the fact that the films were grown at room temperature [8,9].

The diffraction peaks of films In_2O_3 were identified with the crystallographic card JCPDS 00-006-0416. Analyzing the diffractogram of the film deposited with 50 W, there is a very strong crystallographic orientation in the direction (222). However, the film grown at 110 W showed higher crystallinity with a preferential growth in the direction (400). It is also noted that the power increase favored crystallinity, which is also reported by other authors as resultant of the greater kinetic energy of the molecules colliding with the substrate [9-11]. However, in this study, it is worth mentioning that such effect is much more due to the greater thickness of the films deposited with higher power outputs.

Fig. 4 - Diffractograms of thin films manufactured in the sputtering system: a) copper; b) SiO_2; c) In_2O_3 deposited with 50W; d) In_2O_3 deposited with 110W.

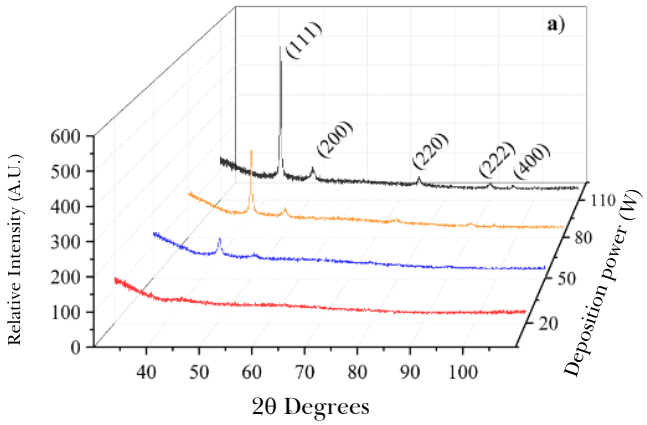

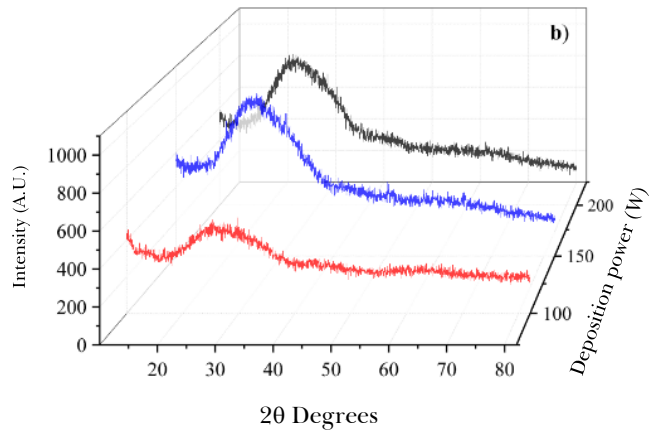

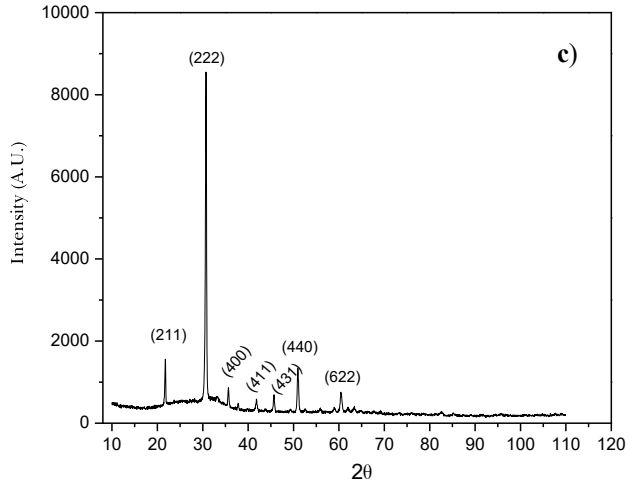

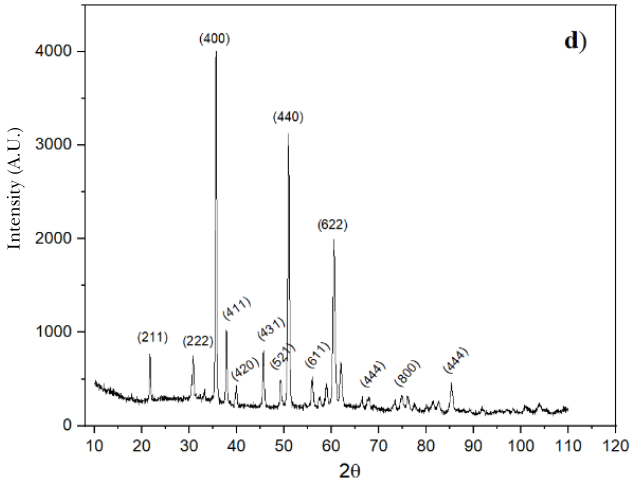

Figures 5 to 7 show atomic force microscopy (AFM) images of the deposited films surface. The roughness values obtained from the respective images are shown in Tables 5 to 7.

The AFM images show that the films are nanometric, and there is a small increase in grain size with power. This result is in accordance with the increase in crystallinity observed in Figure 4, for higher power outputs [12,13].

As for roughness, a small increase is observed in function of the deposition power, a fact that is related to the greater thickness of films deposited with higher power outputs.

Fig. 5 - AFM images of thin copper films deposited with: (a) 20W; (b) 50W; (c) 80W; (d) 110W.

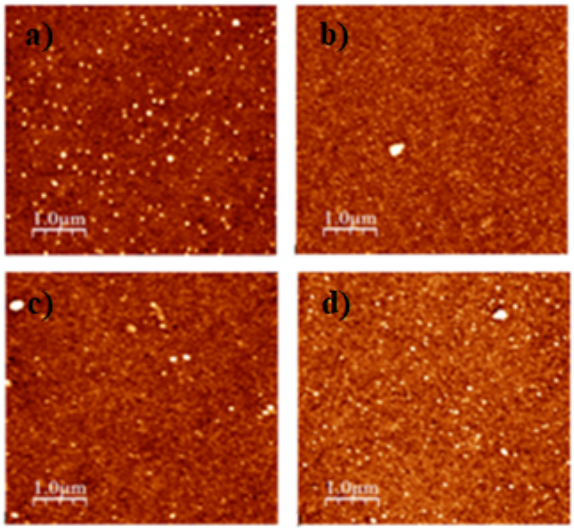

Fig. 6 - AFM images of thin SiO_2 films deposited with: (a) 100W; (b) 150W.

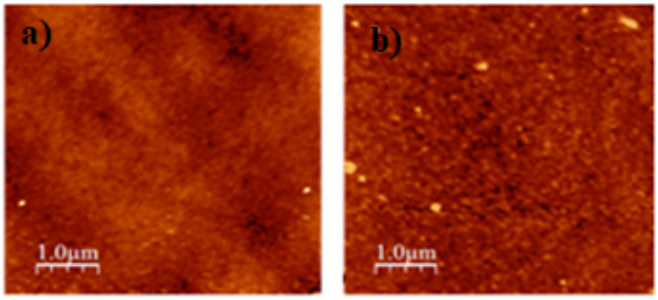

Fig. 7 - AFM images of thin films of In_2O_3 deposited with: (a) 50W; (b) 110W.

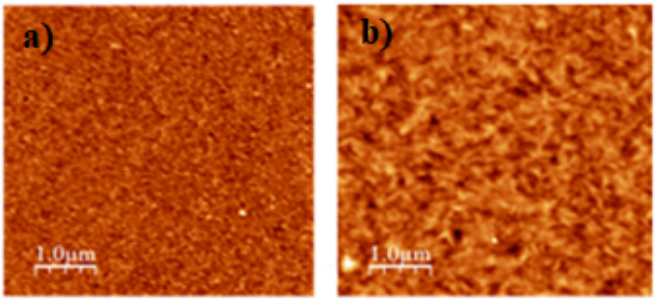

Table 5 - Roughness of thin copper films in function of deposition power.

POWER (W)	ROUGHNESS (nm)
20	1.58
50	1.71
80	1.85
110	1.36

Table 6 - Roughness of thin SiO_2 films in function of the deposition power.

POWER (W)	ROUGHNESS (nm)
100	0.65
150	0.94

Table 7 - Roughness of thin In_2O_3 films in function of the deposition power.

POWER (W)	ROUGHNESS (nm)
50	0.65
110	0.94

Figure 8 shows the variation in the resistivity of the copper and In_2O_3 films in function of the deposition power. The resistivity of the silicon oxide films was not measured, since the film was insulating. The measured values are in the same order of magnitude as the reported resistivity of the materials: 1.7 $\mu\Omega$.cm for copper [14], and 4.0 x 10^{-4} Ω.cm for In_2O_3 films [15, 16]. This result also contributes to attest to the good control of the deposition parameters in the assembled system.

The transmittance curves of SiO_2 and In_2O_3 films deposited in the different power outputs are shown in Figure 9. Since copper is a metal, the transmittance of the film was not measured.

By analyzing the transmittance spectra of In_2O_3 films, a variation in the position of the fundamental absorption edge of the films is observed in relation to the power. This result is well reported in the literature as a consequence of the formation of oxygen vacancies [17].

Analyzing the transmittance spectrum of the SiO_2 film deposited at 100W, it is noted that its behavior resembles the spectrum of silica with an absorbing edge at the end of the visible spectrum. This result is consistent with the amorphous characteristic of SiO_2 deposited with this power. However, the spectra of thin films produced at 150 and 200 W show that the fundamental absorption edges were extended to the near-ultraviolet region, which is a characteristic of SiO_2 crystalline (quartz). These results are consistent with the trend towards crystallization observed in the respective AFM images (Figure 6) of the films deposited with higher power outputs.

Fig. 8 - Electrical resistivity of thin films manufactured in the sputtering system in function of deposition power: a) copper; b) In_2O_3.

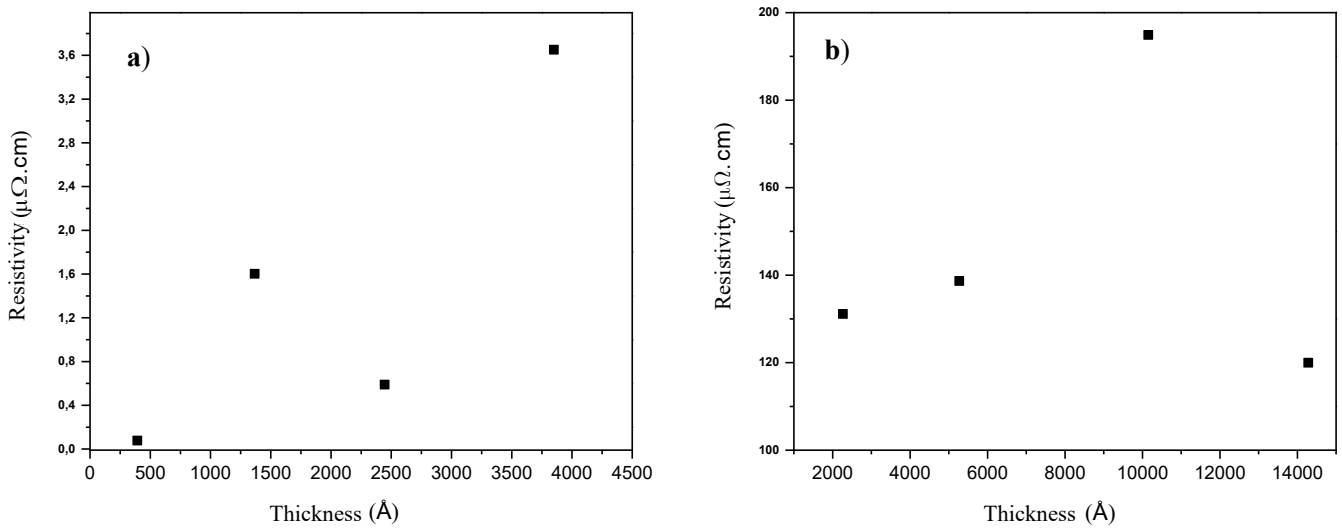

Fig. 9 - Transmittance spectra of thin films manufactured in the sputtering system at different power outputs: a) In_2O_3 thin films; b) SiO_2 thin films.

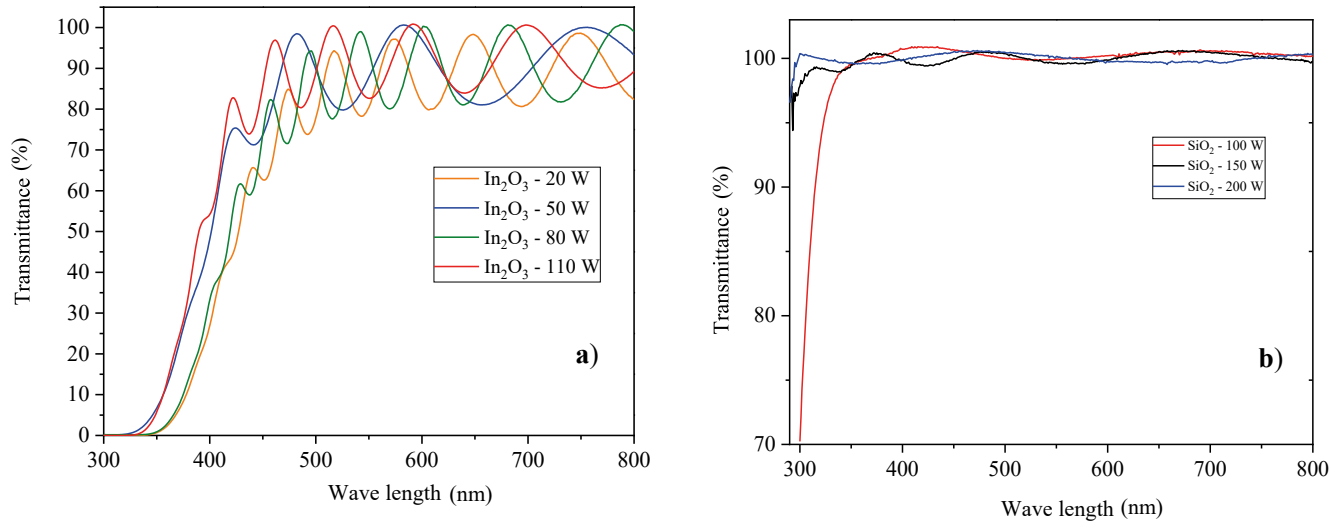

4 Conclusions

A radio frequency magnetron sputtering system was designed and assembled for the manufacture of thin films. This system is operational on the LFF-IME installations, having already performed more than 60 deposition cycles. The depositions of the three targets with different characteristics (conductor, semiconductor, and insulator) provided films of good quality, good thickness uniformity, and properties similar to those reported in the literature. The deposition rate of films varied linearly in relation to work power. These experimental results attest that the assembled system provides good control of deposition parameters.

Acknowledgments

The authors thank the War Arsenal of Rio de Janeiro (AGR) and the Mechanical Workshop of the Brazilian Center for Research in Physics (CBPF) for their readiness in modeling and machining for the assembly of the deposition system. The authors also thank the Materials Division of the National Institute of Metrology, Standardization and Industrial Quality (INMETRO), which collaborated for the characterization of the manufactured films, and the Coordination for the Improvement of Higher Education Personnel (CAPES), for the financial support.

References

[1] KELLY, P. J.; ARNELL, R. D. Magnetron sputtering: a review of recent developments and applications. Vacuum, Amsterdam, v. 56, n. 3, p. 159-172, 2000.
[2] GÜRAKAR, S.; HORZUM, T. Serin, Variation of structural and optical properties of TiO2 films prepared by DC magnetron sputtering method with annealing temperature, Materials Science & Engineering B, 262. Ancara: Universidade de Ancara, 2020.
[3] DEPLA, K.; STRIJCKMANS, R. de G. The role of the erosion groove during reactive sputter deposition, Surface & Coatings Technology, [s. l.], v. 258, p. 1011-1015, 2014.
[4] CRUZ, L. R.; LOPES, B. F. M.; MEDEIROS, R. A.; LIMA, R. M. C.; FERREIRA, C. L. Propriedades de filmes finos de ZnO:Al depositados sobre substratos de poliimida à temperatura ambiente para aplicações em dispositivos optoeletrônicos flexíveis. Cerâmica, [s. l.], v. 63, n. 366, p. 162-168, 2017.
[5] HELL, J.; HORKEL, M.; NEUBAUER, E.; EISENMENGER-SITTNER, C. Construction and characterization of a sputter deposition system for coating granular materials. Vacuum, Amsterdam, v. 84, 453–457, 2010.
[6] SINGH, M. M.; VIJAYA, G.; KRUPASHANKARA, M. S.; SRIDHARA, B.K.; SHRIDHAR, T. N. Deposition and Characterization of Aluminium Thin film Coatings using DC Magnetron Sputtering Process. Materials Today: Proceedings, Amsterdam, v. 5, n. 1, p. 2696-2704, 2018.
[7] BHORDE, A. et al. (400)-Oriented indium tin oxide thin films with high mobility and figure of merit prepared by radio frequency magnetron sputtering, Thin Solid Films, [s. l], v. 704, p. 137972, 2020.
[8] KARTHIKEYAN, S.; HILL, A. E.; PILKINGTON, R. D. The deposition of low temperature sputtered IN2O3 films using pulsed d.c. magnetron sputtering from a powder target. Thin Solid Films, [s. l], v. 550, p. 140-144, 2014.
[9] SCHURIG, P.; COUTURIER, M.; BECKER, M.; POLITY, A.; KLAR, P. Optimizing the Stoichiometry of Ga2O3 Grown by RF-Magnetron Sputter Deposition by Correlating Optical Properties and Growth Parameters, Phys. Status Solidi A, [s. l], v. 216, 1900385, 2019.
[10] MELLO, A. Filmes finos cristalinos de hidroxiapatita: Uma abordagem original com magnetron sputtering de Alvos Opostos. 2007. Tese (Doutorado) - Instituto Militar de Engenharia, Rio de Janeiro, 2007.
[11] CHOI, K H.; KANG, H. C. Structural and optical evolution of Ga2O3/glass thin films deposited by radio frequency magnetron sputtering. Materials Letters, [s. l], v. 123, p. 160-164, 2014.
[12] AMALATHAS, P.; ALKAISI, M. Effects of film thickness and sputtering power on properties of ITO thin films deposited by RF magnetron sputtering without oxygen. Journal of Materials Science: Materials in Electronics, [s. l], v. 27, 2016
[13] THILIPAN, G.; RAO, A. Influence of power on the physical and electrical properties of magnetron sputtered gadolinium oxide thin films for MOS capacitors. Materials Science in Semiconductor Processing, v. 121, 105408, 2021.
[14] QUADROS, H. B. Avaliação das características resistivas de filmes finos absorvedores de radiação eletromagnética. 2014. Trabalho (Conclusão de Curso em Engenharia Aeroespacial) - Universidade Federal de Santa Catarina, Santa Catarina, 2014.
[15] BERRY, P. M.; HALL, M. T. Thin films technology. New York: Van Nostrand Reinhold Company publication, 1968.
[16] CRUZ, L. R. et al. Análise comparativa das propriedades de óxidos transparentes condutores para aplicação em células solares de filmes finos de CdTe. Matéria, v. 22, n. 1, e11793, 2017.
[17] KALEEMULLA, S.; REDDY, A. S.; UTHANNA, S.; REDDY, P. S. Physical properties of In2O3 thin films prepared at various oxygen partial ressures, Journal of Alloys and Compounds, [s. l.], v. 479, n. 1–2, p. 589-593, 2009.